A detailed product distribution analysis of some potential energy surfaces describing the OH + CO → H + CO 2 reaction

ARTICLE *in* COMPUTATIONAL AND THEORETICAL CHEMISTRY · JUNE 2012

Impact Factor: 1.55 · DOI: 10.1016/j.comptc.2011.09.039

3 AUTHORS:

Ernesto Garcia
Universidad del País Vasco / Euskal Herriko…
93 PUBLICATIONS **1,137** CITATIONS
SEE PROFILE

Jose C Corchado
Universidad de Extremadura
118 PUBLICATIONS **3,296** CITATIONS
SEE PROFILE

Joaquin Espinosa-Garcia
Universidad de Extremadura
141 PUBLICATIONS **2,186** CITATIONS
SEE PROFILE

Computational and Theoretical Chemistry 990 (2012) 47–52

Contents lists available at SciVerse ScienceDirect

Computational and Theoretical Chemistry

journal homepage: www.elsevier.com/locate/comptc

A detailed product distribution analysis of some potential energy surfaces describing the OH + CO → H + CO_2 reaction

Ernesto García [a,*], José Carlos Corchado [b], Joaquin Espinosa-García [b]

[a] Departamento de Química Física, Universidad del País Vasco, 01006 Vitoria, Spain
[b] Departamento de Química Física, Universidad de Extremadura, 06071 Badajoz, Spain

ARTICLE INFO

Article history:
Received 11 July 2011
Received in revised form 15 September 2011
Accepted 26 September 2011
Available online 6 October 2011

Keywords:
OH + CO reaction
Quasiclassical trajectory
Gaussian binning
Vibrational states
Product distributions

ABSTRACT

An extensive quasiclassical investigation in a quantum spirit of the OH + CO → H + CO_2 reaction on the three most popular potential energy surfaces has been performed. Using the standard, the Gaussian and the one dimensional Gaussian binning techniques, product angular and translational energy distributions were calculated and compared with those obtained from the molecular beam experiments. Such a comparison shows that pseudoquantization methods hardly improve the agreement. An analysis of the convergence of the binning methods on the number of reactive trajectories used to calculate the product distributions was also carried out proving that a huge number of trajectories are needed to obtain accurate results in the Gaussian binning case against a significantly lower number in the standard and one dimensional Gaussian binning procedures. Finally, product vibrational distributions of the CO_2 molecule were also calculated via pseudoquantization of the vibrational energy of products. Unfortunately, experimental data are not available for comparison.

1. Introduction

Theoretical investigation of elementary chemical reactions can probe the accuracy of the potential energy surface (PES) and the dynamics method used by comparing the calculated reaction probabilities to the information available from measured crossed molecular beam (CMB) data [1]. For the title hydroxyl radical – carbon monoxide, OH + CO → H + CO_2, reaction, important for combustion [2,3] and atmospheric chemistry modelling [4,5], a sufficiently large amount of experimental data has been measured. In particular, in the 1990s decade, Casavecchia and coworkers used a CMB apparatus to detect the CO_2 product by mass spectrometry and then deconvoluted the measured distributions in the laboratory angle to evaluate the product center-of-mass (CM) angular (PAD) and translational energy (PTD) distributions at the collision energies (E_{tr}) of 8.6 and 14.1 kcal mol^{-1} [6–8]. The CO_2 PADs evaluated in this way with respect to the OH velocity exhibit a bimodal forward–backward structure with a strong forward bias. The two corresponding PTDs peak at approximately the same product translational energy (E'_{tr} = 28 kcal mol^{-1}) with the low E_{tr} distribution being narrower than that at high E_{tr}.

In the last decade, three full-dimensional ab initio PESs (YMS [9], LTSH [10], Leiden [11]) were developed for the purpose of studying the reactive dynamics of the OH + CO → H + CO_2 reaction. These PESs exhibit several stationary points and multiple reaction paths. In particular, they exhibit two deep wells, associated with the cis and trans HOCO radicals which are stable enough to react with atmospheric atoms, molecules and radicals [12] or to carry out photodetachment studies [13,14].

On these PESs, several kinetics and dynamics theoretical studies, mainly of quasiclassical trajectory (QCT) type, were carried out [15–36]. Some quantum calculations either of the reduced dimensionality type [17–20] or limited to null total angular momentum [25–30] were also performed. Kinetically, when comparing theoretical results with experimental information, QCT estimates of the rate coefficients show a significant underestimation of the measured data at low temperatures and an overestimation at the high ones. Dynamically, QCT integral cross sections, calculated in the range of collision energy considered by the experiment [37], also underestimate strongly the measured values. In addition, the calculated QCT CM product distributions do not reproduce the results of the CMB experiment with the CM PTDs being significantly narrower than the measured ones and peaking at lower translational energy. Theoretical CM PADs calculated on the YMS and LTSH PESs show, indeed, a bimodal forward–backward structure as the experimental ones, although their structure is more pronounced and more symmetric. On the contrary, the Leiden CM PADs are largely isotropic. To make the comparison unique the theoretical CM PADs and PTDs were transformed into the corresponding laboratory angular distributions (LADs) [36]. The theoretical LADs show a bimodal structure clearly differing from the rather

* Corresponding author.
E-mail address: e.garcia@ehu.es (E. García).

2210-271X/$ - see front matter © 2011 Elsevier B.V. All rights reserved.
doi:10.1016/j.comptc.2011.09.039

unimodal with a shoulder structure of the experimental distribution. Even more, by taking in consideration the experimental conditions (beam velocity distributions, angular divergences, detector aperture) to transform the QCT CM product distributions to the laboratory ones, the comparison between the theoretical and the experimental distributions is still unsatisfactory [38].

As a further attempt to investigate the source of such discrepancies, in this paper we have analyzed the use of different ways of discretizing the (continuous) internal energy of the formed products, *i.e.*, we have superimposed a "quantum spirit" to the quasiclassical description of the dynamics. Several methods to deal with pseudoquantization of the rotational and vibrational components of the classical internal energy of products and, more in particular, with the zero point energy (ZPE) problem have been proposed [39–55]. Pseudoquantization procedures have shown that the agreement between QCT and experimental results can be improved significantly (see for example Refs. [56,57]).

The aim of the present paper is to investigate the influence of different pseudoquantization procedures on the product angular, translational and vibrational energy distributions of the $OH(v_{OH} = 0, j_{OH} = 0) + CO(v_{CO} = 0, j_{CO} = 0)$ reaction at $E_{tr} = 14.1$ kcal mol^{-1}, in order to improve its agreement with the CMB results. Accordingly, the paper is organized as follows: in Section 2, the details of the QCT calculations and the PESs are presented; in Section 3, the procedures used to calculate the vibrational states of the product CO_2 molecules and to weight the reactive trajectories are discussed; Section 4 shows the product translational and angular distributions obtained on the different PESs using the different procedures to weight the reactive trajectories as well as the comparison with the CMB experimental results; in Section 5, an investigation on the convergence of the distributions on the number of reactive trajectories used to calculate them is carried out; in Section 6, product vibrational distributions calculated on the different PESs are discussed, and finally Section 7 draws the main conclusions.

2. The computational machinery

The calculations were performed on the YMS, LTSH and Leiden PESs. The YMS and LTSH PESs are of the Many-Body Expansion (MBE) type [58] whose parameters are determined by fitting ab initio accurate electronic energies and then adding various Gaussians to enforce the reproduction of some local structures of the ab initio data. On the contrary, the Leiden PES is based on the Shepard interpolation of a set of ab initio electronic energy values together with their first and second derivatives. In the Shepard method the potential energy associated with an arbitrary geometry is calculated as a weighted sum of Taylor expansions (truncated to the second order) centered on the different points of the ab initio data (1250 in this case). This makes the computation associated with the Leiden PES significantly more expensive (about 100 times) than that associated with the YMS and LTSH ones.

The QCT calculations were performed at $E_{tr} = 14.1$ kcal mol^{-1} and at the ground ro-vibrational states of both OH and CO using the program VENUS96 [59]. The value of the maximum impact parameter was set to 2.8 Å for the YMS and LTSH PESs and to 2.2 Å for the Leiden PES. Initial and final distances were set at 8.0 Å, a distance large enough to consider negligible the interaction between the fragments of the related channels. All remaining parameters (vibrational phases and spatial orientation of molecules) were selected randomly.

An integration step of 0.01 fs was used for the Leiden PES leading to a error in the conservation of total energy typically lower than 2×10^{-4} kcal mol^{-1}. As known [10,34], a poor conservation of total energy was found for trajectories calculated on the YMS and LTSH PESs. This feature implied to fix a tolerance limit to energy deviation so that trajectories exceeding this limit were discarded. This limit was set to the same value chosen for cutting the long range tail of the potential, *i.e.*, ±0.04 kcal mol^{-1} being this value stricter than those used in previous investigations [10]. Moreover, due to the large tolerance allowed in the integration of trajectories on the YMS and LTSH PESs, an integration step as large as 0.24 fs could be used in these cases.

For YMS and LTSH PESs the number of calculated trajectories was 50×10^6 and 250×10^6, respectively, so that, after the discarding of the unstable trajectories, there were still one million of reactive events left in both cases. For the Leiden PES, one million of reactive events required the integration of 210×10^6 trajectories. Moreover, additional 22×10^9 trajectories (with more than 450×10^6 reactive events) were calculated on the YMS PES in order to improve the convergence of the pseudoquantization methods. The integration of such a large number of trajectories was made possible by the use on the Grid of GEMS (Grid Empowered Molecular Simulator) [60–62]. The simulator exploits the potentialities of high throughput computing on the grid platform deployed within the European Grid Initiative [63] and made available to the Virtual Organization COMPCHEM [64,65].

3. The binning methods for the determination of vibrational state populations

To assign a discrete quantum-like vibrational state to the outcome of a classical trajectory we used the normal mode analysis algorithm (NMA) [66]. This choice was motivated by its lower computational cost against the fast Fourier transform method [67] yielding similar results. The basic idea of the NMA method is to project the final coordinates and momenta of the reactive trajectories onto the respective normal-mode space. It is thus possible to calculate subsequently the kinetic, the potential and the vibrational energy for each mode. From the vibrational energy the harmonic vibrational action x_i for each mode i (the CO_2 molecule involves four modes that correspond to the symmetric and antisymmetric stretchings and to the two degenerate bendings) can then be obtained. Harmonic vibrational actions are obviously continuous numbers and therefore need to be quantized in order to confer a quantum spirit to the quasiclassical results. In fact, Borh quantization indicates that only integer actions are permitted and consequently to calculate the final quantities only trajectories starting with reactants with integer actions and ending with products with integer actions have to be taken into account. However, the set of trajectories ending with exactly integer actions is null. The alternative is to assign a weight in the statistics to each trajectory such that the closer the final actions to integer values, the larger the weights. Several procedures were adopted for assigning statistical weights to trajectories depending on their harmonic vibrational actions. The theoretical arguments of such procedures applied to reactions with products with several vibrational degrees-of-freedom can be found in Ref. [43].

The first procedure is the standard binning (SB), or histogram procedure, in which each trajectory contributes with a weight equal to one to populate the quantum state associated with the nearest integers to the different vibrational actions $\{x_i\}$ of the already mentioned i modes. In other words, the SB weight is a delta function of the difference of the actions with respect to the nearest integers $\bar{x}_i$ and subsequently each trajectory ending in the CO_2 molecule with vibrational actions in the interval $(\bar{x}_i - 0.5, \bar{x}_i + 0.5)$ contributes to the statistics with weight equals to one.

The second procedure used is the Gaussian binning (GB) developed by Bonnet and coworkers [39–43,56,57]. In this procedure, the weight, $W^{GB}(\{x_i\})$, of a trajectory to populate the $\{\bar{x}_i\}$ state is not one. It is instead defined as:

$$W^{GB}(\{x_i\}) = \prod_i \frac{1}{\pi^{1/2}\varepsilon} \exp\left[-\frac{1}{\varepsilon^2}(x_i - \bar{x}_i)^2\right] \quad (1)$$

where the weight assigned to the various vibrational action values x_i is a Gaussian function of $(x_i - \bar{x}_i)$, that is, a Gaussian centered at the nearest (integer) state $\bar{x}_i$. It is also necessary to mention here that we consider that one trajectory only contributes to one quantum vibrational state. As usual the ε coefficient was set equal to 0.05 [41,56,57,68,69]. Thus the Gaussian weight is characterized by a full width at half maximum of about 10% and therefore the action values ranging from $\bar{x}_i - 0.05$ to $\bar{x}_i + 0.05$ are those that mainly contribute to the population of the level $\bar{x}_i$. As a consequence, it is necessary to run ≈10 times more trajectories per vibrational mode within the GB procedure that within the SB one for the same level of convergence of final results. So, for the CO_2 molecule, one is led to run $\approx 10^4$ times more trajectories with the GB procedure.

The third procedure used (developed in Refs. [52,53] and called here one dimensional Gaussian binning (1GB) as in Ref. [43]) obviates this problem by pseudoquantizating the total vibrational energy instead of the vibrational actions. Then the weight, $W^{1GB}(\{x_i\})$, of a trajectory to populate the $\bar{x}_i$ state reads as:

$$W^{1GB}(\{x_i\}) = \frac{1}{\pi^{1/2}\varepsilon} \exp\left[-\frac{1}{\varepsilon^2}\left(\frac{\sum_i \omega_i (x_i - \bar{x}_i)}{\sum_i \omega_i}\right)^2\right] \quad (2)$$

where ω_i is the harmonic frequency of the ith mode. In this case, the 1GB weight is a Gaussian function of the difference of the harmonic energies. The 1GB procedure needs many fewer trajectories than the GB procedure for the same level of convergence of the final results and therefore it allows a significant computational saving.

4. The resulting product translational and angular distributions

Fig. 1 shows the QCT PTDs calculated on the YMS (top panel), LTSH (central panel) and Leiden (bottom panel) PESs. In each panel also the experimental values of Refs. [6–8] are shown for comparison as a solid line and a hatched area for its uncertainty. The distributions have been obtained using a histogram method for translational energy with bins of 2 kcal mol^{-1} and normalized to the maximum. SB and 1GB PTDs are shown as dotted and dashed lines respectively without error bars. In both cases the standard deviation is always lower than the 1% and the resulting curves are smooth. PTDs calculated using the GB procedure are shown as solid circles with the related error bars.

As apparent from Fig. 1, for all the PESs there is an excellent agreement between the SB and the 1GB results. This means that given that the number of trajectories is large, the SB and 1GB methods are well suited to exploit the product phase space information. This is obviously favoured by the large exoergicity of the process (−23.5 kcal mol^{-1}) and the high density of the product states due to the heavy mass of the CO_2 molecule. On the contrary, the GB results for the LTSH and Leiden PESs are affected by large statistical errors in spite of the large number of reactive trajectories calculated. The associated error may, in fact, be as large as the 70%. To reduce this error a larger number of reactive trajectories are needed. This has been performed on the YMS PES where the error has been reduced to the 5% and the GB curve became smooth. It is worth to note that the GB PTD is slightly hotter than those calculated using the SB and 1GB methods.

However, regardless of the method used the PTDs calculated on the three PESs clearly disagree with the experiment. They are, in fact, largely symmetric (the value of the average product translational energy coincides with that of the maximum of the distribution) while the experimental data is definitely shifted to higher product translational energy. This difference can be explained because the theoretical average fraction of translational energy for

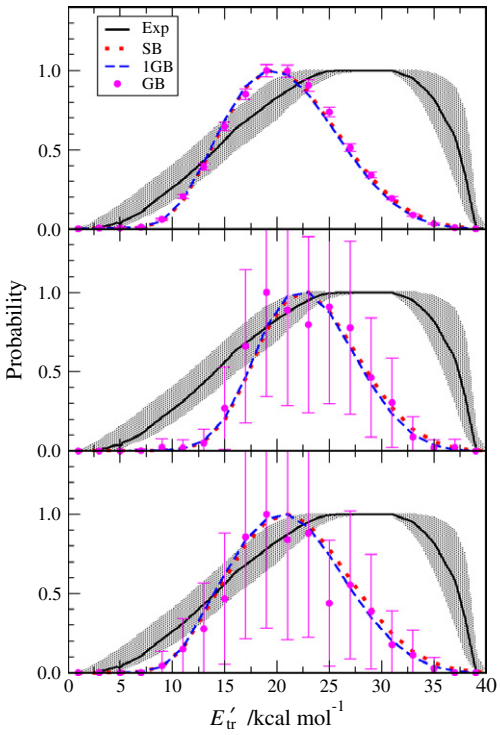

Fig. 1. QCT product translational energy distributions for the OH($v_{OH} = 0, j_{OH} = 0$) + CO($v_{CO} = 0, j_{CO} = 0$) reaction at $E_{tr} = 14.1$ kcal mol^{-1} calculated on the YMS (top panel), LTSH (central panel) and Leiden (bottom panel) PESs by using the standard (SB) (dotted line), one dimensional (1GB) (dashed line) and Gaussian (GB) (circles) binning procedures. Error bars are shown only when they are significant. Experimental values of Refs. [6–8] are given as a solid line. Hatched areas represent the experimental uncertainty. Distributions are normalized to the maximum.

the three PESs underestimates the experimental value: 0.53, 0.61 and 0.59 for the YMS, LSTH and Leiden surfaces, respectively, against 0.64 for experiment [7]. This smaller fraction of translational energy is related with an insufficient repulsive character in the topology of the reaction path in the exit channel for the three surfaces, which represents a limitation of these surfaces for dynamics studies. Obviously, the underestimation of the translational energy leads to overestimation of the internal energy in the products, mainly in the vibrational energy available for the products. This point will be analyzed later in the product vibrational distribution (PVD) case.

QCT PADs calculated on the YMS (top panel), LTSH (central panel) and Leiden (bottom panel) PESs are plotted in Fig. 2 together with the experimental ones [6–8]. The distributions have been obtained using a histogram method for scattering angle with bins of 10° and normalized to the maximum. As in Fig. 1, SB and 1GB results are shown as continuous curves (standard deviations are smaller than the 1.5%) and GB results as solid circles with the error bars (for the LTSH and Leiden PESs the errors are even larger than those of the PTD ones). The higher error corresponds to the smaller and the larger scattering angle due to the amplification factor of the division by the sine of the angle needed to obtain the differential cross section in solid angle.

As apparent from the figure, there is again a good agreement between SB and 1GB results for all the PESs even in the wings of the distributions where, as just mentioned, the error becomes larger because of the division of the sine of the angle. The comparison between the PAD curve obtained with the GB method on the YMS PES and those calculated using the SB and 1GB procedures shows slight discrepancies, mainly in the backward region. Theoretical distributions however differ from the experiment. In fact, even though the

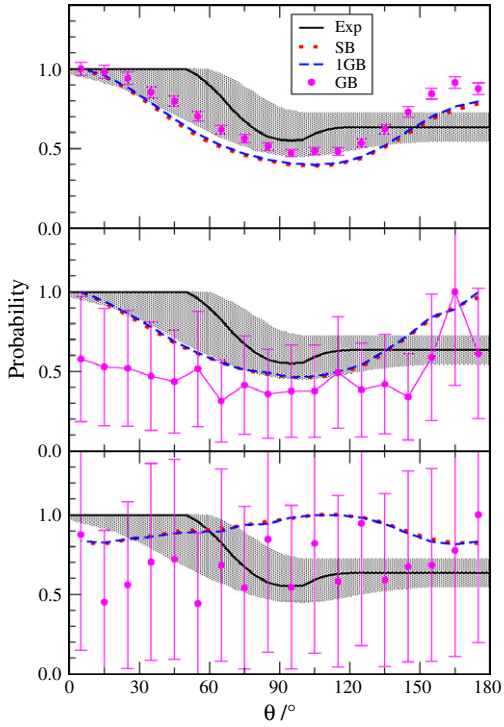

Fig. 2. QCT product angular distributions for the OH($v_{OH} = 0, j_{OH} = 0$) + CO($v_{CO} = 0, j_{CO} = 0$) reaction at $E_{tr} = 14.1$ kcal mol^{-1} calculated on the YMS (top panel), LTSH (central panel) and Leiden (bottom panel) PESs by using the standard (SB) (dotted line), one dimensional (1GB) (dashed line) and Gaussian (GB) (circles) binning procedures. Error bars are shown only when they are significant. Experimental values of Refs. [6–8] are given as a solid line. Hatched areas represent the experimental uncertainty. Distributions are normalized to the maximum.

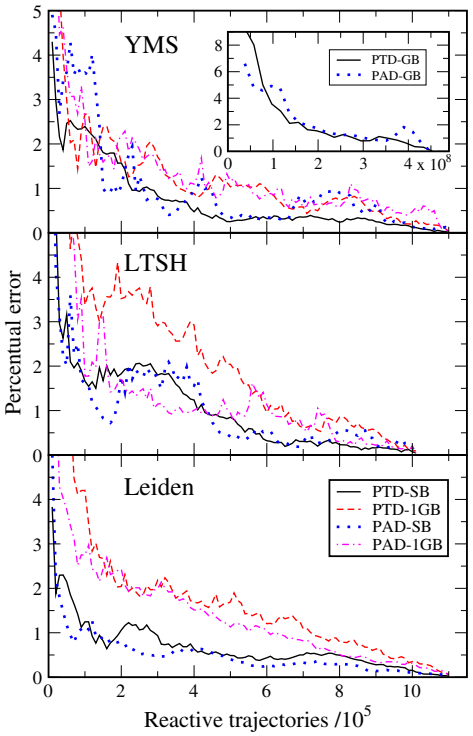

Fig. 3. Percentual error of the PTD and PAD as a function of the number of reactive trajectories for the OH($v_{OH} = 0, j_{OH} = 0$) + CO($v_{CO} = 0, j_{CO} = 0$) reaction at $E_{tr} = 14.1$ kcal mol^{-1} calculated on the YMS (top panel), LTSH (central panel) and Leiden (bottom panel) PESs by using the standard (SB) and one dimensional (1GB) binning procedures. Inserted graph over the top panel, idem for the Gaussian binning (GB) procedure.

YMS and LTSH PADs almost fall within the experimental uncertainty, they are more symmetric than the experimental values. On the other hand, the Leiden PADs are clearly sideways.

5. The convergence of the distributions

In order to investigate in more detail the behavior of the product distributions calculated using the above mentioned methods we determined their rate of convergence as the number of reactive trajectories increases. Fig. 3 shows as a function of the reactive trajectories considered in the calculation the percentual error of the product translational and angular distributions with respect to the overall values. The SB and 1GB results are considered for the three PESs and the GB ones for the YMS PES because the statistics for the LTSH and Leiden GB cases is too poor.

As apparent from the figure, there is a clear convergence as the number of reactive trajectories increases irrespectively of the PES and of the binning method. However, some differences are apparent. In fact, distributions calculated using the SB method converge faster than the 1GB ones. This feature is a consequence of the Gaussian weight of Eq. (2) which decreases significantly the "number of reactive events" to be considered. Also the velocity of convergence depends on the used PES. In particular, convergences on the LTSH is slower than those on the other PESs. Thus, for instance, on the LTSH PES an error lower of the 2% needs more than 3.0×10^5 reactive trajectories for the PTD when the SB method is applied while this value increases to 5.2×10^5 in the 1GB case. On the contrary, the YMS and Leiden PESs favour a faster convergence because only 1.4×10^5 and 0.6×10^5 reactive trajectories are necessary to achieve errors lower than 2% for the PTD in the SB case and 2.8×10^5 and 3.3×10^5 trajectories in the 1GB one.

Convergence of both PTD and PAD when the GB pseudoquantization method is applied becomes much more difficult. In fact, as shown in Fig. 3, 1.6×10^8 reactive trajectories are required to achieve errors lower than 2% for both PTD and PAD.

Therefore we conclude that the SB and 1GB results can be converged within the limits of a non very expensive QCT treatment and, as a consequence, can be used also as a predictive tool. On this ground they are used in the next section to argue about the product vibrational distributions.

6. The resulting product vibrational distributions

The QCT PVDs calculated using the SB method on the YMS (top panel), LTSH (central panel) and Leiden (bottom panel) PESs are plotted in Fig. 4. The distributions have been obtained by assigning each vibrational action calculated by using the NMA method [66] to its nearest integer and only the most populated vibrational states are shown. Vibrational states are denoted by (n_1, n_2, n_3), being n_1 the symmetric stretching mode, n_2 the bending mode, and n_3 the antisymmetric stretching mode. It is worth to mention here that the vibrational states in Leiden PVD are shifted to larger energies because the harmonic frequencies of CO_2 are slightly larger.

As apparent from the figure, the most populated vibrational states are those with relatively large bend excitation. For example, the states with maximum population for the YMS, LTSH and Leiden are, respectively, (0, 5, 0), (0, 4, 0) and (0, 4, 0) and even states with 11 quanta in the bending mode are significantly populated. Also states excited in the bending mode and with one, two or even three quanta in the symmetric stretching mode are populated. Less likely are product molecules with excited antisymmetric stretching

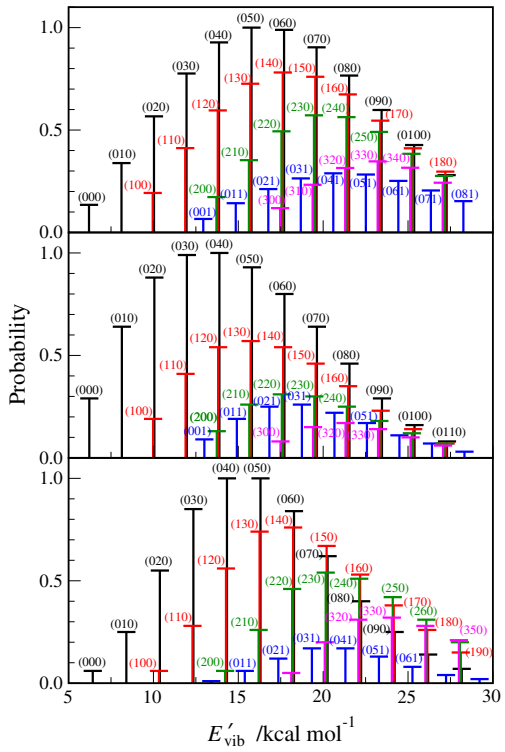

Fig. 4. QCT product vibrational distributions for the OH(v_{OH} = 0, j_{OH} = 0) + CO(v_{CO} = 0, j_{CO} = 0) reaction at E_{tr} = 14.1 kcal mol^{-1} calculated on the YMS (top panel), LTSH (central panel) and Leiden (bottom panel) PESs using the SB procedure. Vibrational states are denoted by (n_1, n_2, n_3), being n_1 the symmetric stretching mode, n_2 the bending mode, and n_3 the antisymmetric stretching mode. Distributions are normalized to the maximum.

mode. In fact, in this case only the first excitation occurs and it is accompanied by excitation in the bending mode. The main difference between the PVDs calculated on the three PESs is that the YMS PVD is hotter than the LTSH and Leiden ones (in agreement with the fact that the YMS PTD peaks at low product translational energy). Other important differences are the different relative populations along the vibrational progressions. Thus the (0, n_2, 0) progressions, *i.e.* the vibrational progressions on the bending mode, indicate that the LTSH tends to populate the vibrational states with n_2 lower than the corresponding to the maximum population while the Leiden PES tends to populate vibrational states with n_2 higher. This latter behavior is even more evident for the YMS PES for which states with values of n_2 as higher as 11 continue to be notably populated.

Theoretical PVD for the OH(v_{OH} = 0, j_{OH} = 0) + CO(v_{CO} = 0, j_{CO} = 0) → H + CO_2 reaction at E_{tr} = 13.8 kcal mol^{-1} on the LTSH PES was also reported in Ref. [10]. There are some differences between that PVD and the one calculated by us on the same PES, which merit be commented. Thus the maximum vibrational state populated in Ref. [10] is the (1, 3, 0) one versus the (0, 4, 0) state in our results. Also states with one, two and three quanta in the bending mode (0, n_2, 0) have a similar population than the (1, 3, 0) one in results of Ref. [10]. If additional excitation in the bending mode is added, $n_2 > 3$, the population of such states decreases much faster than in our results. Such differences can be attributed, besides the slight difference in collision energy (13.8 versus 14.1 kcal mol^{-1}), to the filter used to discard non-conserving total energy (much stricter in our case). To test this possibility we have recalculated the PVD using a filter of 2.24 kcal mol^{-1} (instead of 0.04 kcal mol^{-1}), similar to that used in Ref. [10]. The new PVD slightly differs from the old one being somewhat cooler. As a consequence, the differences between the PVDs calculated in Ref. [10] and in the present paper have to be attributed to the different number of reactive events (10^4 trajectories before the discarding procedure in Ref. [10] and 2.7×10^6 trajectories after the discarding procedure in the present paper). Note that the different methods to calculate the vibrational actions (a fast Fourier transform as implemented in the ACTION program [67] in Ref. [10] and the NMA method of Ref. [66] here) cannot be ruled out, although two of us [66] demonstrated that both methods yield similar results.

So far product vibrational distributions obtained applying the SB method were considered. In order to complete the analysis PVDs have been also calculated using the 1GB method. Resulting PVDs do not differ significantly from the SB ones regardless the potential surface used. In fact, the application of the 1GB procedure leads to PVDs with slightly smaller populations of the vibrational states with high values of the bending quantum number though the discrepancies are always lower than the 7%. The differences are also smaller when the bending quantum number is low. Moreover, the GB PVD calculated on the YMS PES is slightly cooler than those obtained using the SB and 1GB methods, as expected from its hotter PTD.

However, before the end of this section we would like to point out two remarkable observations. First, in the above analysis of the PTD we found that the three PESs underestimate the experimental average fraction of energy released as product translational energy, $\langle f'_{tr} \rangle$, between 3% and 11%, and consequently they will probably overestimate the average fraction of energy as vibration, $\langle f'_{v} \rangle$. The latter value is 0.32, 0.22 and 0.22 for the YMS, LSTH and Leiden surfaces, respectively. With a total available energy of about 40 kcal mol^{-1}, the average energy available for vibration is 12.8, 8.8 and 8.8 kcal mol^{-1}, respectively. So, assuming that this energy goes to the bending mode, the center of the vibrational distribution would be at the (0,6,0), (0,4,0) and (0,4,0) states, respectively, which are very close to the most populated vibrational levels according to Fig. 4. It is therefore quite possible that experimental vibrational distributions peak at somewhat lower excited states. Second, another effect that could contribute to a higher population of highly excited vibrational states is related to the zero point energy problem associated with QCT calculations [39–55]. Although we have used pseudoquantization approaches to correct the QCT classical limitations, this criterion is applied only to the final product, not along the trajectory, and so the conservation of the ZPE per mode is not guaranteed, allowing unphysical energy transfer between modes. Therefore, we conclude that due to the few repulsive character of the exit channel described by the three surfaces and to the non-conservation of the ZPE per mode, the PVDs are overestimated and cooler vibrational distributions should be expected.

7. Conclusions

An analysis of the outcomes of a QCT study of the title reaction has allowed us to investigate the properties of the PTDs, PADs and PVDs of the OH(v_{OH} = 0, j_{OH} = 0) + CO(v_{CO} = 0, j_{CO} = 0) reaction at E_{tr} = 14.1 kcal mol^{-1} on different PESs and using different discretization approaches. In particular, it was found that the shape, the agreement with the experimental data, and the convergence of the calculated distributions significantly vary both with the PES used and with the methods of assigning QCT outcomes to the discrete quantum states. We have found in fact that calculated PTDs systematically disagree (they are significantly cooler) with the experiment regardless of the PES used, and that calculated PADs clearly discriminates between the outcomes of the Leiden PES from those of the other two. We have also found that for both, the calculated PTDs and PADs the SB and the 1GB results can be con-

verged with a relatively small number of reactive trajectories. However, this number of reactive trajectories leads to GB results statistically unsatisfactory. In this case it is necessary to provide a huge number of reactive events in order to obtain acceptable errors. This has been checked only for the YMS PES and the calculated GB PTDs and PADs do not differ significantly from the SB and 1GB results. Moreover, the analysis of the rate of convergence of the SB and 1GB distributions on the number of reactive trajectories used to calculate them shows a slower convergence of the 1GB method and when the LTSH PES is considered. On the other hand, regardless the potential surface, PVDs show a clear predilection to populate highly excited bending states both without and with excitation in the stretching modes. Like in the case of the PTDs and PADs, SB PVDs are slightly modified when the 1GB and GB procedures are applied. This fact is clearly a consequence of the large number of vibrational states available to the products and therefore the energetic gap between them will be small, moving the system away from the quantum regime. Unfortunately, no information is available from the CMB experiment to compare with. Nor it is possible to compare the calculated PVDs with data of Ref. [70] because such experiment was performed at room temperature (in that experiment, by the way, the estimated fraction of energy available as product vibration is 6% and only bend excitation was observed). We hope, however, that the results dicussed here prompt further experimental work useful for a comparison with theory.

Acknowledgments

We thank Professor Antonio Laganà for helpful discussions. This work has been supported by the Spanish MICINN (CTQ2008-025878/BQU) and Junta de Extremadura (Project Number IB10001). Computer time allocation has been obtained from the COMPCHEM VO of EGI.

References

[1] N. Balucani, G. Capozza, F. Leonori, E. Segoloni, P. Casavecchia, Int. Rev. Phys. Chem. 25 (2006) 109.
[2] J. Warnatz, U. Maas, R.W. Dibble, Combustion: Physical and Chemical Fundamentals, Modeling and Simulation, Experiments, Pollutant Formation, fourth ed., Springer-Verlag, Berlin, 2006.
[3] J.A. Miller, R.J. Kee, C.K. Westbrook, Annu. Rev. Phys. Chem. 41 (1990) 345.
[4] R.P. Wayne, Chemistry of Atmospheres, Oxford Univ. Press, Oxford, 2000.
[5] B.J. Finlayson-Pitts, J.N. Pitts, Chemistry of the Upper and Lower Atmosphere Theory, Academic Press, London, 2000.
[6] M. Alagia, N. Balucani, P. Casavecchia, D. Stranges, G.G. Volpi, J. Chem. Phys. 98 (1993) 8341.
[7] M. Alagia, N. Balucani, P. Casavecchia, D. Stranges, G.G. Volpi, J. Chem. Soc. Faraday Trans. 91 (1995) 575.
[8] P. Casavecchia, N. Balucani, G.G. Volpi, in: K. Liu, A. Wagner (Eds.), The Chemical Dynamics and Kinetics of Small Radicals, World Scientific, Singapore, 1996, p. 365.
[9] H.G. Yu, J.T. Muckerman, T.J. Sears, Chem. Phys. Lett. 349 (2001) 547.
[10] M.J. Lakin, D. Troya, G.C. Schatz, L.B. Harding, J. Chem. Phys. 119 (2003) 5848.
[11] R. Valero, M.C. van Hemert, G.J. Kroes, Chem. Phys. Lett. 393 (2004) 236.
[12] J.H. Francisco, J.T. Muckerman, H.G. Yu, Acc. Chem. Res. 43 (2010) 1519.
[13] C.J. Johnson, R.E. Continetti, J. Phys. Chem. Lett. 1 (2010) 1895.
[14] C.J. Johnson, B.L.J. Poad, B.B. Shen, R.E. Continetti, J. Chem. Phys. 134 (2011) 171106.
[15] J.M. Bowman, G.C. Schatz, Annu. Rev. Phys. Chem. 46 (1995) 169.
[16] K. Kudla, G.C. Schatz, in: K. Liu, A. Wagner (Eds.), The Chemical Dynamics and Kinetics of Small Radicals, World Scientific, Singapore, 1995, p. 438.
[17] D.C. Clary, G.C. Schatz, J. Chem. Phys. 99 (1993) 4578.
[18] M.I. Hernández, D.C. Clary, J. Chem. Phys. 101 (1994) 2779.
[19] E.M. Goldfield, S.K. Gray, G.C. Schatz, J. Chem. Phys. 102 (1995) 8807.
[20] D.H. Zhang, J.Z.H. Zhang, J. Chem. Phys. 103 (1995) 6512.
[21] N. Balakrishnan, G.D. Billing, J. Chem. Phys. 104 (1996) 4005.
[22] F.N. Dzegilenko, J.M. Bowman, J. Chem. Phys. 108 (1998) 511.
[23] G.D. Billing, J.T. Muckerman, H.G. Yu, J. Chem. Phys. 117 (2002) 4755.
[24] R. Valero, G.J. Kroes, J. Chem. Phys. 117 (2002) 8736.
[25] D.A. McCormack, G.J. Kroes, Chem. Phys. Lett. 352 (2003) 281. Erratum, Chem. Phys. Lett. 373 (2003) 648.
[26] D.M. Medvedev, S.K. Gray, E.M. Goldfield, M.J. Lakin, D. Troya, G.C. Schatz, J. Chem. Phys. 120 (2004) 1231.
[27] Y. He, E.M. Goldfield, S.K. Gray, J. Chem. Phys. 121 (2004) 823.
[28] R. Valero, D.A. McCormack, G.K. Kroes, J. Chem. Phys. 120 (2004) 4263.
[29] R. Valero, G.J. Kroes, Phys. Rev. A 70 (2004) 040701.
[30] R. Valero, G.J. Kroes, J. Phys. Chem. A 108 (2004) 8672.
[31] R. Valero, G.J. Kroes, Chem. Phys. Lett. 417 (2006) 43.
[32] S. Zhang, D.M. Medvedev, E.M. Goldfield, S.K. Gray, J. Chem. Phys. 125 (2006) 164312.
[33] X. Song, J. Li, H. Hou, B. Wang, J. Chem. Phys. 125 (2006) 094301.
[34] E. Garcia, A. Saracibar, L. Zuazo, A. Laganà, Chem. Phys. 332 (2007) 162.
[35] H.Y. Sun, C.K. Law, J. Mol. Struct. – THEOCHEM 862 (2008) 138.
[36] E. Garcia, A. Saracibar, A. Laganà, Theor. Chem. Acc. 128 (2011) 727.
[37] S. Koppe, T. Laurent, H.R. Volpp, J. Wolfrum, P.D. Naik, in: 26th Symp (Int) on Combustion, The Combustion Institute, Pittsburgh, 1996, p. 489.
[38] A. Laganà, N. Balucani, S. Crocchianti, P. Casavecchia, E. Garcia, A. Saracibar, Lect. Notes Comput. Sci. 6784 (2011) 453.
[39] L. Bonnet, J.C. Rayez, Chem. Phys. Lett. 277 (1997) 183.
[40] L. Bonnet, J.C. Rayez, Chem. Phys. Lett. 397 (2004) 106.
[41] L. Bonnet, J. Chem. Phys. 128 (2008) 044109.
[42] L. Bonnet, Chin. J. Chem. Phys. 22 (2009) 210.
[43] L. Bonnet, J. Espinosa-García, J. Chem. Phys. 133 (2010) 164108.
[44] A.J.C. Varandas, J. Chem. Phys. 99 (1993) 1076.
[45] A.J.C. Varandas, Chem. Phys. Lett. 225 (1997) 18.
[46] A.J.C. Varandas, Int. Rev. Phys. Chem. 19 (2000) 199.
[47] A.J.C. Varandas, L. Zhang, Chem. Phys. Lett. 340 (2001) 62.
[48] A.J.C. Varandas, Chem. Phys. Lett. 439 (2007) 386.
[49] W.H. Miller, W.L. Hase, C. Darling, J. Chem. Phys. 91 (1989) 2863.
[50] J.M. Bowman, B. Gazdy, Q.Y. Sun, J. Chem. Phys. 91 (1989) 2859.
[51] Z. Xie, J.M. Bowman, J. Phys. Chem. A 110 (2006) 5446.
[52] G. Czakó, J.M. Bowman, J. Chem. Phys. 131 (2009) 244302.
[53] G. Czakó, A.L. Kaledin, J.M. Bowman, J. Chem. Phys. 132 (2010) 164103.
[54] M. González, A. Saracibar, E. Garcia, Phys. Chem. Chem. Phys 13 (2011) 3421.
[55] M. González, J. Mayneris-Perxachs, A. Saracibar, E. Garcia, Phys. Chem. Chem. Phys. 13 (2011) 13638.
[56] M.L. González-Martínez, L. Bonnet, P. Larrégaray, J.C. Rayez, J. Chem. Phys. 126 (2007) 041102.
[57] J. Espinosa-García, L. Bonnet, J.C. Corchado, Phys. Chem. Chem. Phys. 12 (2010) 3873.
[58] J.N. Murrell, S. Carter, S.C. Farantos, P. Huxley, A.J.C. Varandas, Molecular Potential Energy Functions, Wiley, Chichester, 1984.
[59] W.L. Hase, R.J. Duchovic, X. Hu, A. Komornicki, K.F. Lim, D. Lu, G.H. Peslherbe, K.N. Swamy, S.R. Van de Linde, A.J.C. Varandas, H. Wang, R.J. Wolf, QCPE Bull. 16 (1996) 43.
[60] A. Laganà, in: A. Laganà, G. Lendvay (Eds.), Theory of the Dynamics of Elementary Molecular Reactions, Kluwer Academic, Dordrecht, 2004, p. 363.
[61] A. Costantini, O. Gervasi, C. Manuali, N. Faginas-Lago, S. Rampino, A. Laganà, J. Grid Comput. 8 (2010) 571.
[62] S. Rampino, A. Monari, S. Evangelisti, E. Rossi, K. Rud, A. Laganà, in: M. Bubak, M. Turala, K. Wiatr (Eds.), Proceedings of the Cracow'09 Grid Workshop, ACC CYFRONET AGH, Cracow, 2010. ISBN:9788361433019.
[63] European Grid Infrastructure. <http://www.egi.eu> (accessed 24.06.11).
[64] A. Laganà, A. Riganelli, O. Gervasi, Lect. Notes Comput. Sci. 3980 (2006) 665.
[65] Computational Chemistry (COMPCHEM) Virtual Organization. <http://www.compchem.unipg.it> (accessed 24.06.11).
[66] J.C. Corchado, J. Espinosa-García, Phys. Chem. Chem. Phys. 11 (2009) 10157.
[67] G. Schatz, Comput. Phys. Commun. 51 (1988) 135.
[68] L. Bañares, F.J. Aoiz, P. Honvault, B. Bussery-Honvault, J.M. Launay, J. Chem. Phys. 118 (2003) 565.
[69] L. Bonnet, C. Crespos, Phys. Rev. A: At. Mol. Opt. Phys. 78 (2008) 062713.
[70] M.J. Frost, P. Sharkey, I.W.M. Smith, Faraday Discuss. Chem. Soc. 91 (1991) 305.